ABSTRACT

Influence of Rapamycin on Zea Mays Seedlings

Chi T. Nguyen

Director: Bryan Gibbon, Ph.D.

The Target of Rapamycin (TOR) Signal Transduction Pathway is a conserved mechanism that plays a significant role in the regulation of cell growth. Autophagy inhibition is one method in which the TOR kinase pathway is able to regulate cellular energy balance. Rapamycin is a known inhibitor of the TOR kinase pathway, and thus is expected to increases autophagic activity in the cellular system. This study was conducted to examine this inductive effect of rapamycin on autophagic recycling in W64A+ maize seedlings. In order to conduct the experiment, maize seedlings were treated with varying concentrations of rapamycin in DMSO solution followed by a week length observation of root growth. Although there was evidence of increased root growth in moderate concentrations of rapamycin (30 nM), no statistically significant trend was found. Elevated autophagy gene expression involved in the nutritional stress response for increased root growth was analyzed through cDNA samples of the harvested seedlings roots. However, dysfunctional ATG gene primers prevented complete analysis of the autophagic expression in the rapamycin treated W64A+ seedlings.

APPROVED BY DIRECTOR OF HONORS THESIS:

_____

Dr. Bryan Gibbon, Department of Biology

APPROVED BY THE HONORS PROGRAM

_____

Dr. Andrew Wisely, Director

DATE:_____

INFLUENCE OF RAPAMYCIN ON ZEA MAYS SEEDLINGS

A Thesis Submitted to the Faculty of

Baylor University

In Partial Fulfillment of the Requirements for the

Honors Program

By

Chi Nguyen

Waco, Texas

May 2013

TABLE OF CONTENTS

LIST OF FIGURES AND TABLES

ACKNOWLEDGEMENTS

First and foremost, I would like to thank my thesis director, Dr. Bryan Gibbon, for his constant support, mentoring, and patience in developing the project and guiding me through it to the end, as well as allowing me the opportunity to work in his lab. I would also like to give my appreciation to Mo Jia and Hao Wu for their technical assistance and continuous support in the lab. And much thanks to the Baylor University College of Arts and Sciences and the Department of Biology for graciously funding the required materials for my experiment. Lastly, I would furthermore like to acknowledge Dr. Tamarah Adair and Dr. Jonathan Tran for their professional insight and patience in reviewing my thesis.

CHAPTER ONE

Literature Review

Target of Rapamycin Signal Transduction Pathway

The target of Rapamycin (TOR) Kinase Pathway is a conserved pathway that plays a role in regulation of cell growth through a signal transduction cascade. This pathway regulates growth through external input signals such as nutrient availability, stress, energy level, and different growth factors that can either stimulate or repress cell growth and proliferation through the action of the serine/threonine protein kinase TOR (Rohde et al., 2001). TOR signaling regulates cell growth by selective translation of mRNAs and regulated transition through the G_1/S phase of cell cycle. Therefore, environmental cues such as nutrient availability, stress, energy balance, and growth factors will allow TOR signaling to respond in such a way that will regulate ribosome synthesis, translation, and transcription of genes involving in the translational machinery that will coordinate survival, growth, and cell development in all eukaryotes (Dennis et al., 1999). In response to external environmental cues, the TOR pathway helps the cell regulate energy balance, thus ensuring its survival in varying environmental conditions. The primary class of growth factors involved in TOR signaling transduction is insulin or insulin-like growth factors (IGFs), that serve as important selective activators for mechanisms involving in cell growth regulation such as protein synthesis and ribosome biogenesis, all extensively studied in mammals and yeast (Chung et al., 1992). A diagram of the TOR signaling cascade is summarized below in Figure 1.

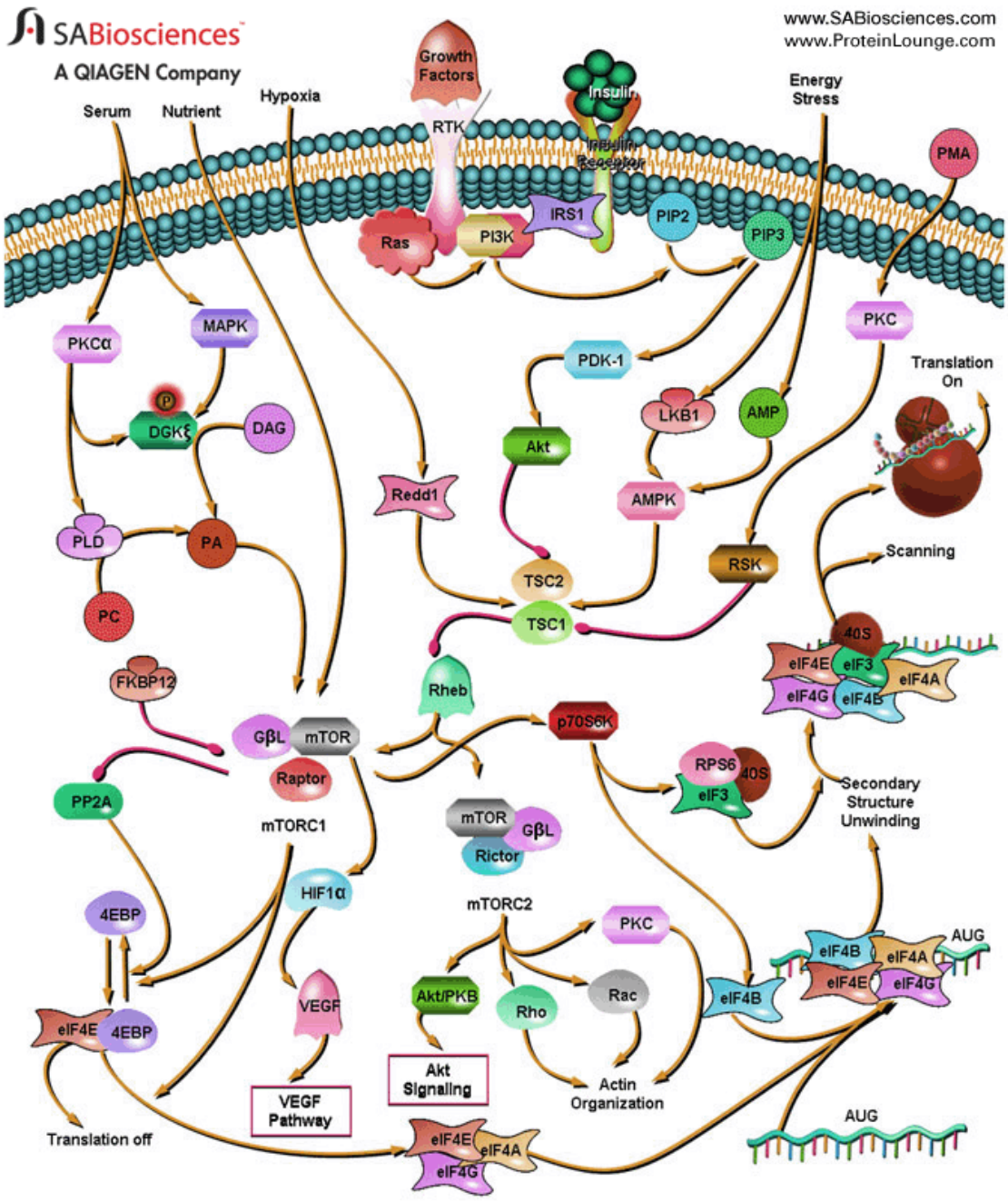

Figure 1: Diagram from SABiosciences illustrating TOR-S6K pathway in mammals. Factors such as nutrient availability, growth factors, insulin, hypoxia, and energy stress can initiate a signaling cascade through phosphorylation of kinases (primarily TOR and S6K), exerting control over growth and protein synthesis by targeting ribosome synthesis. Phosphorylation of TOR (gray) and S6K1 (red) result in increased translation of messages containing the 5A TOP motifs, while dephosphorylation of TOR and S6K1 inhibit translation of such mRNAs. Yellow arrowheads indicate activation and pink round heads indicate inhibition. Image Source: *http://www.sabiosciences.com/pathway.php?sn=mTOR_Pathway*

In response to amino acids, insulin, glucose, or incoming nutrients, the PI3K/AKT transduction pathway (Phosphatidylinositol -3-Kinase/ v-Akt-Murine Thymoma-Viral Oncogene Homolog-1) mediates the activating signal to TOR. TOR signaling is then activated by the formation of the ternary complex TORC1 (Target of Rapamycin Complex1) and TORC2 (TOR Complex 2). TORC1 is rapamycin sensitive and consists of TOR, RAPTOR (regulatory associated protein of TOR), and G-BetaL (G-protein Beta-subunit-like protein). TORC1 is an important effector in the regulation of growth and cellular mass. The rapamycin insensitive TORC2, on the other hand, contains Rictor instead of RAPTOR, and controls cellular structure by regulation of actin cytoskeleton. Activated TOR kinase can control mRNA translation through phosphorylation of ribosomal S6 kinase 1 (S6K1), an important effector downstream of TOR. When phosphorylated by an activated TOR kinase, S6K1, in turn, can phosphorylate and activate the 40S ribosomal S6 protein, resulting in increased preferential translation of mRNAs containing the 5A-Terminal Oligopyrimidine (5A TOP) motif, which is commonly associated with ribosomal proteins, elongation factors, and Insulin-like Growth Factor-II (IGF-II). Inhibition of TOR kinase, alternatively, would dephosphorylate S6K1, resulting in reduced protein translation (Fumarola et al., 2005).

While the TOR signaling transduction pathway has been well characterized in non-photosynthetic eukaryotes, research involving this signaling pathway in plants are not as extensive. This lack of data on the plant TOR pathway is due to the lack of molecular and biochemical assays for endogenous TOR protein kinase activity and the embryo lethality of null *Arabidopsis* TOR mutants (Dobrenel et al., 2011). However, it is still likely that TOR pathway plays a key role in plants due to the fact that plants are

constantly subjected to stress conditions throughout their life cycle, such as osmotic or nutritional stresses. Research has shown that glucose availability drives TOR signaling to control root meristem activation to regulate growth (Xiong and Sheen, 2012). Identification of the specific regulatory mechanism of TOR in plants is the primary interest of this research.

In plant species, we are particularly interested in the TOR homologs in maize. Research had identified and characterized various orthologs of TOR and the ribosomal protein S6K1 in maize TOR signaling (Agredano-Moreno et al., 2007). In plants, S6K2 is hypothesized to be an ortholog of the mammalian S6K due to its observed function of ribosomal S6 protein phosphorylation. The S6K homologs are first identified in the model plant *Arabidopsis*, originally referred to as ATPK6 and ATPK19, which later on become S6K1 and S6K2 (Zhang et al., 1994). So far, experiments with *Arabidopsis thaliana* have identified both TOR and RAPTOR (RAPTOR1/RAPTOR2) plant homologs that have previously been identified in the mammalian TOR pathway, and these experiments suggest the possible role of TOR in embryo development and meristem-driven cell growth (Anderson et al., 2005). Later research demonstrated that the *Arabidopsis* phosphoinositide-dependent kinase-1 (PDK1) activity is not inhibited by osmotic stress treatment (Mahfouz set al., 2006). PDK1 is a protein kinase that is involved in a variety of processes including cell proliferation, differentiation, and apoptosis, thus indicating that osmotic stress inhibition of S6K in plants is likely to be mediated through the TOR kinase pathway.

Rapamycin: Regulation and Function

Rapamycin, a macrocyclic lactone, is a natural antibiotic produced by a soil bacterium *Streptomyces hyproscopicus* that also possess immunosuppressive, antifungal, and antitumor properties. In the yeast model, rapamycin inactivates the TOR kinase pathway by binding to TOR and FKBP12. This interaction forms noncovalent bonds between the FKBP12 (a peptidyl-prolyl isomerase originally characterized as a cytosolic receptor for rapamycin) and the FRB (FKBP12-Rapamycin Binding) domains of TOR protein to produce a specific FKBP12/Rapamycin protein complex that functions in mimicking the nutritional stress signal, thus inducing recycling of cell components through the autophagy process (Harding et al., 1989).

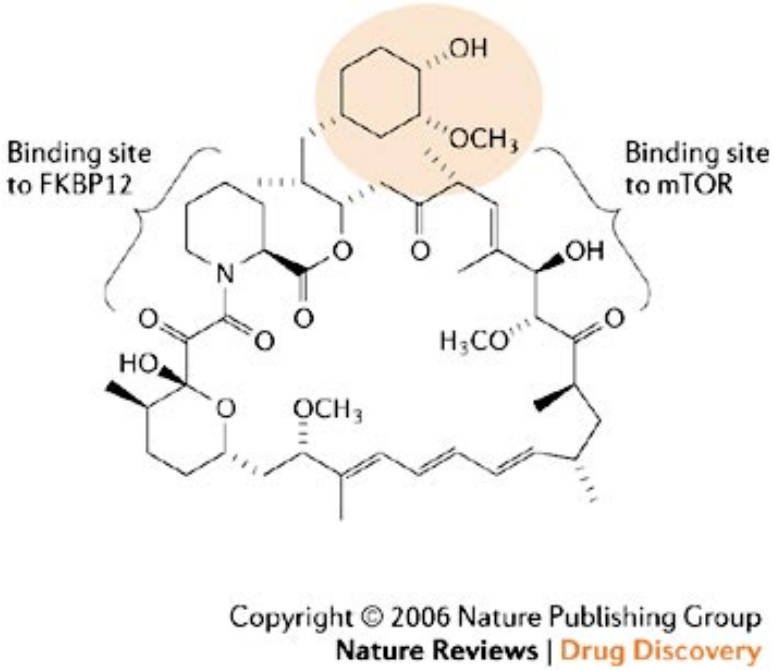

Figure 2: Molecular structure of Rapamycin. Retrieved from online web source (Faivre, 2006).

The inhibitory effects of the FKBP12/rapamycin complex on TOR kinase function is suggested to occur either by dissociation of RAPTOR from TOR or by blockage of a specific subset of TORC1 (Target of Rapamycin Complex1) substrates

(Oshiro et al., 2004). In response to nutrient cues from the environment, TORC1 inhibits stress responses and regulates cellular growth (Loewith et al., 2011). In the rapamycin signaling pathway occurring in mammalian models, an initial complex is first formed from binding of rapamycin to FKBP12, which then binds to mTOR (mechanistic target of rapamycin). However, unlike yeasts and mammals, a study with *Arabidopsis* suggested that some plants may be insensitive to rapamycin; normal physiological levels of rapamycin shown to be effective in inhibiting growth in mammal and yeasts did not exert the same effect on *Arabidopsis* plants. A yeast two hybrid study proposed that evolutionary changes of *Arabidopsis* FKP12's structure maybe responsible for its reduced affinity toward the formation of an inhibitory complex with TOR and rapamycin (Menand et al., 2002). However, unlike *Arabidopsis thaliana*, maize TOR is not resistant to rapamycin; biochemical analyses indicates that *Zea mays* FKBP12 is able to form a functional structure capable of targeting TOR protein kinase (Agredano-Moreno et al., 2007). Rapamycin regulation is therefore conserved in *Zea mays*.

TOR's Function in Autophagy

In this experiment, we are interested in the process by which TOR signaling inhibits autophagy expression to coordinate cell growth and nutrient availability. Autophagy, a highly conserved and regulated catabolic process, is responsible for degradation of cellular components through a vacuolar degradation process, and is essential for cell survival during nutrient starvation. TOR kinases are recognized as a negative regulator of autophagy in response to environmental nutrient condition, and autophagy inhibition by TOR kinase pathway can lead to a cascade effects resulting in less programmed cell death (Chang and Neufeld, 2009). When nutrients are available,

TOR and other kinases influence the ATG1/ATG13 kinase complex by overexpressing phosphorylation of Autophagy 13 (ATG13) subunit, while inhibiting hypophosphorylation of the ATG1 subunit, preventing assembly of the complex and its accessory subunits. In a nutrient-poor environment, inhibition of TOR will prevent ATG13 phosphorylation and induce ATG1 phosphorylation, thus activating the ATG1/ATG13 kinase complex to allow autophagy to occur (Chang and Neufeld, 2009). Following activation of the autophagy kinase complex, autophagy is induced by a series of steps (Li et al., 2012):

1. Delivery of lipids to the developing phagophore by the expression of ATG9
2. Autophagosome nucleation which involves addition of PI3P to the phagophore by the action of VPS34 lipid kinase.
3. Lipidation of ATG8 by ATG12 and ATG5/ATG 16 , which seals and decorates the autophagosome with phosphatidylethanolamine
4. The transportation step of the autophagosome is carried out by the FYVE and FYCO (coiled-coil domain-containing proteins), which attaches the autophagosome to the microtubule transport system to bring the autophagosome to the vacuole.
5. The autophagosome is then partly fused with the tonoplast that will allow autophagic bodies release into the vacuole, resulting in degradation of the vesicles through vacuolar hydrolases mechanism.

The autophagy process is down regulated by activation of the TOR kinase, a catalytic component of TORC1, and certain types of drug, such as rapamycin, can inhibit this TOR activation, which may allow induction of the autophagy process.

Rapamycin's Autophagy Induction through TOR Inhibition

A past study on the TOR inhibition effects on the model green alga *Chlamydomonas reinhardtii* by rapamycin exposure demonstrated increased vacuole size that indicated increased autophagic-processes resulting from nutrient deprivation stimulus (Crespo et al., 2005). It is therefore in our interest to learn more about the mechanism in which rapamycin inactivate the TOR pathway that will lead to autophagy in *Zea mays*, which has shown conservation in TOR signaling. We aimed to analyze the presence of elevated autophagy expression typically involved in the induction of a nutritional stress response. This analysis was carried out by examining the common maize bred line W64A+ seedling root growth in a medium containing variable concentrations of rapamycin, and examining the expression of autophagy genes from the collected seedling roots.

Preliminary experiments conducted in the lab indicated increased root growth in seedlings exposed to moderate concentrations of rapamycin, noticeably between 10 nM to 30 nM (Jia, M. unpublished data). The goal of this experiment was to test the validity of this positive correlation between root growth and moderate concentrations of rapamycin and to examine whether there was increased autophagy gene expression associated with the rapamycin treated *Zea mays* seedlings. Increased root growth may be induced as a result of the mimicking of nutrient deprivation by rapamycin's inhibition of TOR. We hypothesized that an induction of root growth in seedlings treated with moderate concentrations of rapamycin is an indication of increased autophagy induction to allow restoration of nutrient status. Rapamycin at higher concentrations, however, is

toxic to plants and thus seedlings were expected to exhibit slower growth at high levels of rapamycin concentration.

CHAPTER TWO

Material and Methods

Plant Materials and Growth Conditions

Seedling and Growth Media Preparation

This experiment was conducted using *Zea mays* wild type kernels from the W64A+ inbred line, grown in 2012 at the World Hunger Relief field, in Elm Mott, Texas. To prevent possible fungal contamination in later growing seedlings, all kernels used for the experiment were sterilized in a 5% bleach solution, followed by LATITUDE^{TM} Seed Treatment (0.22% administered of the total seeds 'weight) prior to germination. After treatment, all maize kernels were planted in growth media.

Germinating W64A+ seedlings were grown in 3 experimental sets of 11 media tubes treated with varying concentrations of rapamycin. For growth media preparation, 2 g Gellan Gum (Phytotechnologies, Product No. G434) and 4 g Chu N6 Basal Salt (Phytotechnologies, Product No. C416) were dissolved in 1 l deionized water. Then, the Gellan Gum/Basal Salt media solution was autoclaved (Cycle 1) along with 33 labeled empty test tubes (20x150mm) and caps.

Rapamycin Treatment

Rapamycin stock solutions (10 μM, 300 μM, 1000 μM) were made by serial dilutions of rapamycin (914.14g/mol) in 99% DMSO (soluble at 200mg/mL). Rapamycin treatments were then performed on each autoclaved media tube by using serial dilutions from the three pre-made rapamycin stocks. Before media addition,

rapamycin was pipetted into 9 out of 11 autoclaved tubes in each experimental set to produce the following rapamycin concentrations: 1-nM, 3-nM, 10-nM, 30-nM, 100-nM, 300-nM, 1000-nM, 3000-nM, 10000-nM. Additionally, two media tubes were used as controls for each of the three experimental sets. For the first control, 150 μL of DMSO (representing the maximum volume of DMSO used to dissolve rapamycin into the media) was added to each of the three experimental sets to account for any effect of the DMSO on the growing seedlings. While DMSO studies indicated no effect on plant growth in low concentrations (0.2% -0.4%), high DMSO concentration of 0.8% has shown to reduce plant growth by 50% in past studies (Schmitz et al., 1969). For the second control, no DMSO was added, and each of the three experimental sets contained only the media and 150 μL of deionized H_2O (no Rapamycin/DMSO). After measuring the rapamycin stocks, 20 ml of media was added and mixed by light swirling and the tubes were capped and stored at 4^{o}C until all *Zea mays* kernels were prepared for germination.

Seedling Germination

Following availability of 33 LATITUDE^{TM} treated *Zea mays* kernels, sterile forceps were used to transfer each kernel into the 33 prepared media-tubes containing varying concentrations of rapamycin under a vented hood to minimize fungal contamination. For dark-induced etiolation, all germinating tubes were wrapped in aluminum foil to protect germinating seeds from light exposure. The rapamycin-treated kernels were allowed to incubate at 25^{o}C for 2 days, or until germination occurs. Germination was indicated by the emergence of the radicle, an embryonic root.

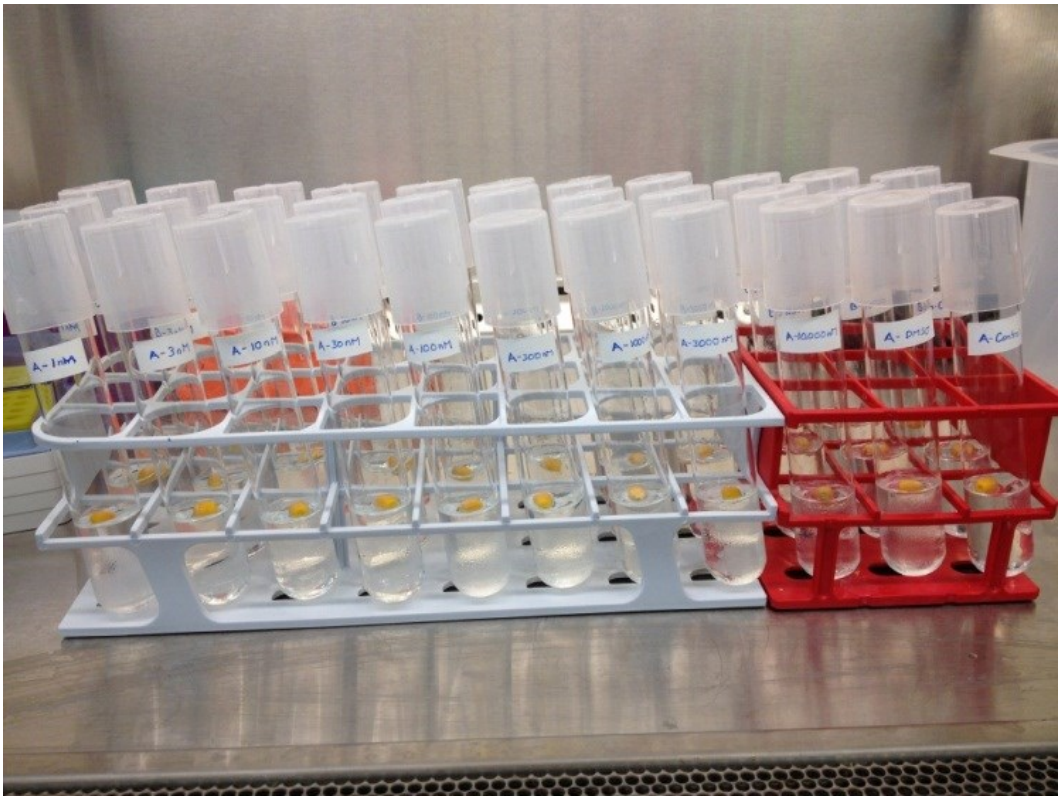

Figure 3: All treated kernels in media growth tubes before germination.

Phenotypic Observation and Measurements

Approximately 30 hours after planting, when seedlings exhibited signs of germination, the aluminum foil was removed for observation and measurements of seedlings' growth. Growth was documented at 2 intervals; the first observation took place on the fourth day after planting, and the second observation took place on the seventh day after planting. Measurements were obtained by taking photographs (using an iPhone camera) of seedlings side by side with a transparent ruler. Phenotypic observations included root elongation, hypocotyl growth, and presence of fungal contamination. All quantitative measurements were performed using ImageJ™, an image processing and analysis software.

Root Elongation

The rate of root growth was the most important phenotypic determinant of autophagy expression, as increased root growth allows increased intake of nutrients from the surrounding environment. Besides increased root elongation, rapamycin's effect in mimicking the starvation response also upregulates autophagy gene expression (Yoshimoto et al., 2004). Therefore, the length and elongation rates of the primary roots were carefully measured during seedlings observation (Wood et al., 2000). Growth rate over time of the primary roots in each tube in correlation with varying concentrations of rapamycin was also compared and analyzed through graphical plots.

Shoot Growth

The procedure also included measurements of *Zea mays* hypocotyl growth for comparison with root growth, as shoot growth is also regulated by glucose availability. With the rapamycin-induced starvation response, the rate of shoot growth is expected to decrease (Xiong and Sheen, 2011). A graph of hypocotyl growth over time versus increasing rapamycin concentrations was also made for comparative analysis with root growth observation.

Fungal Contamination

Despite sterilization and LATITUDE^{TM} treatment, some fungal contamination did occur amongst a percentage of experimental maize seedlings. And since fungal contamination competed with growing seedlings for available nutrient in the media, presence of fungus inhibited seedling growth, and documentation of any contamination

allowed for better data analysis when comparing the root growth expression in varying concentration of rapamycin-affected *Zea mays* seedlings.

Autophagy Gene Expression Analysis

Root RNA Isolation

Seven days after planting, RNA from each root was extracted through *Small Scale RNA Isolation* (which can purify RNA from up to 0.1g of plant tissue) in preparation for later autophagy expression analysis. For this process, root tissues (approximately 0.5mm from tips, where most autophagy occurs), were removed from plants using a sterile razor blade, grounded into powder with a pestle and mortar, and stored in labeled RNAse free microcentrifuge tubes at -70^{o}C. In each of the 33 labeled microcentrifuge tubes containing the frozen plant tissue, RNA extraction from raw roots tissue was performed with Plant RNA Reagent (Life Technologies, Carlsbad, CA).

After RNA isolation, the quantity of the resulting purified root RNA of each microcentrifuge tube was measured using a NanoDrop Spectrophotometer. RNA concentrations (ng/uL) were diluted to the 100-300 ng/uL range, the optimal concentration for downstream RT-PCR processes.

cDNA Preparation

All diluted RNA samples were then converted to cDNA by reverse transcription. Using purified experimental RNA as template, first strand cDNA synthesis was achieved for all available RNA samples using 5x iScript reverse transcriptase supermix, containing iScript MMLV-RT (RNaseH+), Rnase inhibitor, dNTPs, oligo(dT) and random primers, buffer, $MgCl_2$, and stabilizers (Bio-Rad^{TM}). During this procedure, reverse transcription

was carried out in a thermal cycler for 30 minutes at 42^{o}C, followed by reverse transcriptase inactivation for 5 minutes at 85^{o}C. All resulting cDNA *Zea mays* samples were diluted ten-fold with deionized water in preparation for PCR electrophoresis and qPCR.

PCR Electrophoresis

Identification of the proper autophagy-gene specific primers was made using PCR electrophoresis, where annealing activities of different autophagy (ATG) primers were tested on one of the available cDNA *Zea Mays* samples. Using the cDNA as template, a master mix of 10X buffer, $MgCl_2$, dNTP mix, Taq DNA Polymerase, and deionized water were prepared for each ATG primer. The PCR reactions were carried out in a thermal cycler where denaturation first occurred at 95^{o}C for 30s followed by annealing at 59^{o}C for 30s and elongation at 72^{o}C for 1 min. PCR products were subjected to electrophoresis on 1% aragose gel and stained with ethidium bromide. When analyzing the resulting agarose gel, a single DNA fragment indicate a working ATG primer. Each set of ATG primers was measured against a positive RRB1 control, containing forward/reverse RRB1 primers instead of the ATG primers, and a negative control, which contained deionized water instead of the cDNA template.

Real Time qPCR Amplification

If a working ATG primer set was identified from the PCR electrophoresis procedure, the primer set could be used to measure the activity of autophagy gene expression in rapamycin treated *Zea mays* tissues through qPCR amplification assays. Each of the available cDNA samples for all varying concentrations of rapamycin was

used as template for the qPCR reaction, using the 5x iScript supermix with the appropriate ATG primers. In this step, rapamycin treated *Zea mays* cDNA samples that exhibited increased root growth can be measured and analyze for autophagy gene expression using RT-PCR Detection System Rotor-Gene 6000 (QIAGEN^{TM}).

CHAPTER THREE

Data and Results

Phenotypic Observations

The W64A+ seedlings were allowed to germinated in the dark by covering the tubes with aluminum foil, and four days after germination, the growth rate of each maize seedlings in the three sample sets (A, B, C) was observed and documented. The primary observations were measurements of root growth and shoot growth. Measurements were performed by digital image analysis using ImageJ™.

From the data in Table 1, most of the seedlings in each of the three sample sets exhibited significant root growth four days after planting. However, a large number of moldy kernels were observed on many of the growing seedlings, which may have negatively influenced the growth of the young W64A+ seedlings.

Documentation of phenotypic measurements of W64A+ seedlings growth after seven days (Table 2) demonstrated that most seedlings had already outgrown the media tube. Viable and healthy seedlings from each of the three sample set were then harvested for extraction of root tissues. The seedlings samples that did not grow or failed to thrive (labeled as NA) were discarded and not included for the RNA extraction procedure.

Rapamycin Conc. (nM)	Root Growth (cm)	Shoot Growth (cm)	Hypocotyls	Mold
TRIAL A				
No DMSO	8.319	8.227	Y	N
DMSO	6.151	10.77	Y	N
1-nM	NA	NA	N	Y
3-nM	2.121	0.416	N	Y
10-nM	NA	NA	N	Y
30-nM	NA	NA	N	Y
100-nM	1.491	0.406	N	Y
300-nM	0.321	0.268	N	Y
1000-nM	1.771	0.338	Y	N
3000-nM	5.677	2.224	Y	N
10000-nM	NA	NA	N	Y
TRIAL B				
No DMSO	6.482	5.647	Y	N
DMSO	NA	NA	N	Y
1-nM	NA	NA	N	Y
3-nM	5.437	3.669	Y	N
10-nM	4.163	1.486	Y	Y
30-nM	3.575	1.147	Y	Y
100-nM	6.042	4.989	Y	N
300-nM	6.457	3.657	Y	N
1000-nM	1.585	0.0641	Y	N
3000-nM	2.685	1.336	Y	N
10000-nM	1.684	1.112	Y	N
TRIAL C				
No DMSO	NA	NA	N	Y
DMSO	5.682	2.962	Y	N
1-nM	4.085	1.48	Y	Y
3-nM	5.608	3.417	Y	N
10-nM	NA	NA	N	Y
30-nM	8.014	2.459	Y	N
100-nM	4.957	1.533	Y	N
300-nM	NA	NA	N	Y
1000-nM	3.591	2.03	Y	N
3000-nM	NA	NA	N	Y
10000-nM	4.967	4.964	Y	N

Table 1: Measurements taken 4 days after planting on November 16, 2012 using ImageJ™. NA indicated unavailable measurement due to failure of seedlings to germinate or excess mold growth.

Rapamycin Conc. (nM)	Root Growth (cm)	Shoot Growth (cm)	Hypocotyls	Mold
TRIAL A				
No DMSO	9.54	7.264	Y	Y
DMSO	14.268	12.683	Y	N
1-nM	NA	NA	N	Y
3-nM	8.07	4.462	Y	Y
10-nM	NA	NA	N	Y
30-nM	NA	NA	N	Y
100-nM	11.239	7.181	Y	Y
300-nM	4.949	3.083	Y	Y
1000-nM	8.064	5.058	Y	N
3000-nM	9.837	13.21	Y	N
10000-nM	NA	NA	N	Y
TRIAL B				
No DMSO	10.02	17.15	Y	Y
DMSO	NA	NA	N	Y
1-nM	NA	NA	N	Y
3-nM	12.311	16.154	Y	N
10-nM	10.616	10.992	Y	Y
30-nM	12.535	12.575	Y	Y
100-nM	13.587	15.285	Y	N
300-nM	13.026	13.863	Y	N
1000-nM	10.331	10.652	Y	N
3000-nM	10.379	11.256	Y	N
10000-nM	6.291	5.703	Y	N
TRIAL C				
No DMSO	NA	NA	N	Y
DMSO	13.503	13.035	Y	N
1-nM	13.428	12.631	Y	Y
3-nM	12.402	9.544	Y	N
10-nM	NA	NA	N	Y
30-nM	15.985	13.592	Y	N
100-nM	8.358	10.812	Y	N
300-nM	NA	NA	N	Y
1000-nM	9.89	10.915	Y	N
3000-nM	NA	NA	N	Y
10000-nM	8.377	9.882	Y	N

Table 2: Measurements taken 7 days after planting on November 19, 2012 using ImageJ™. NA indicated unavailable measurement due to failure of seedlings to germinate or excess mold growth.

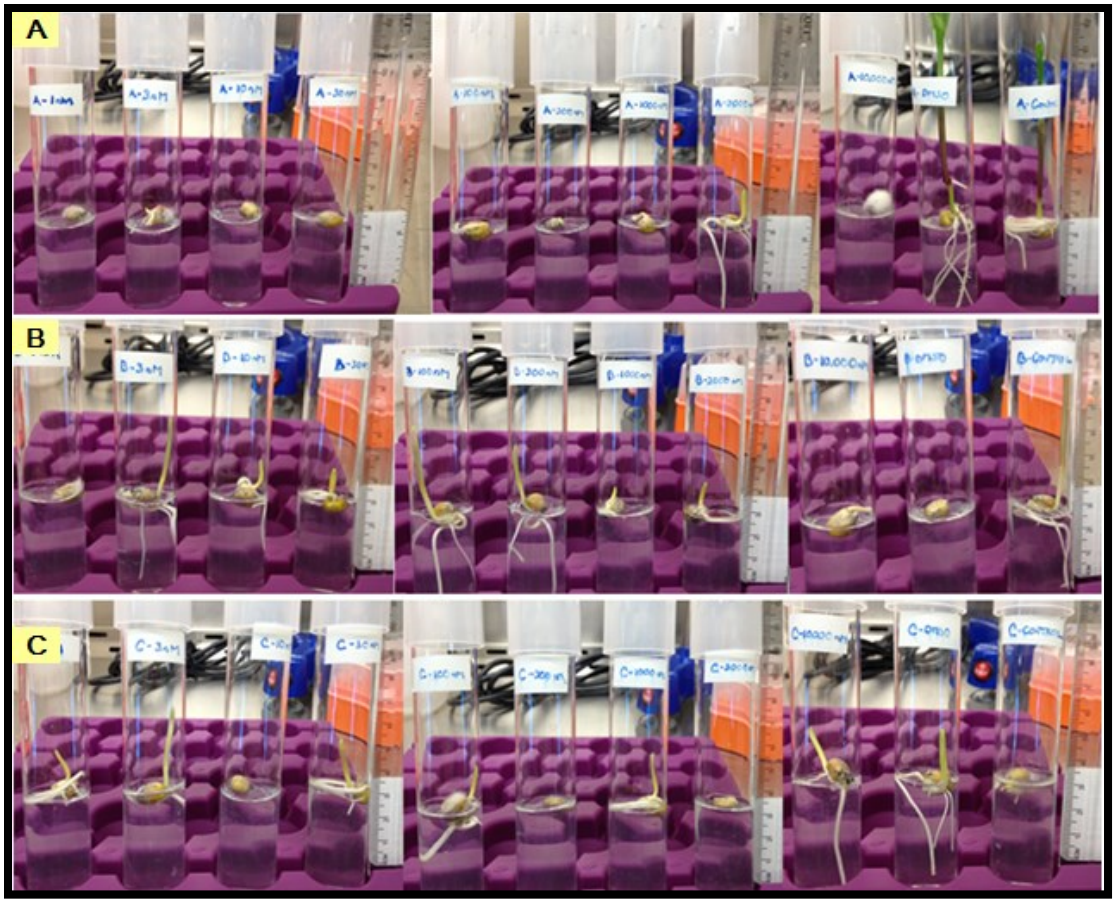

Figure 4: Images taken of the growing W64A+ seedlings 4 days after germination.

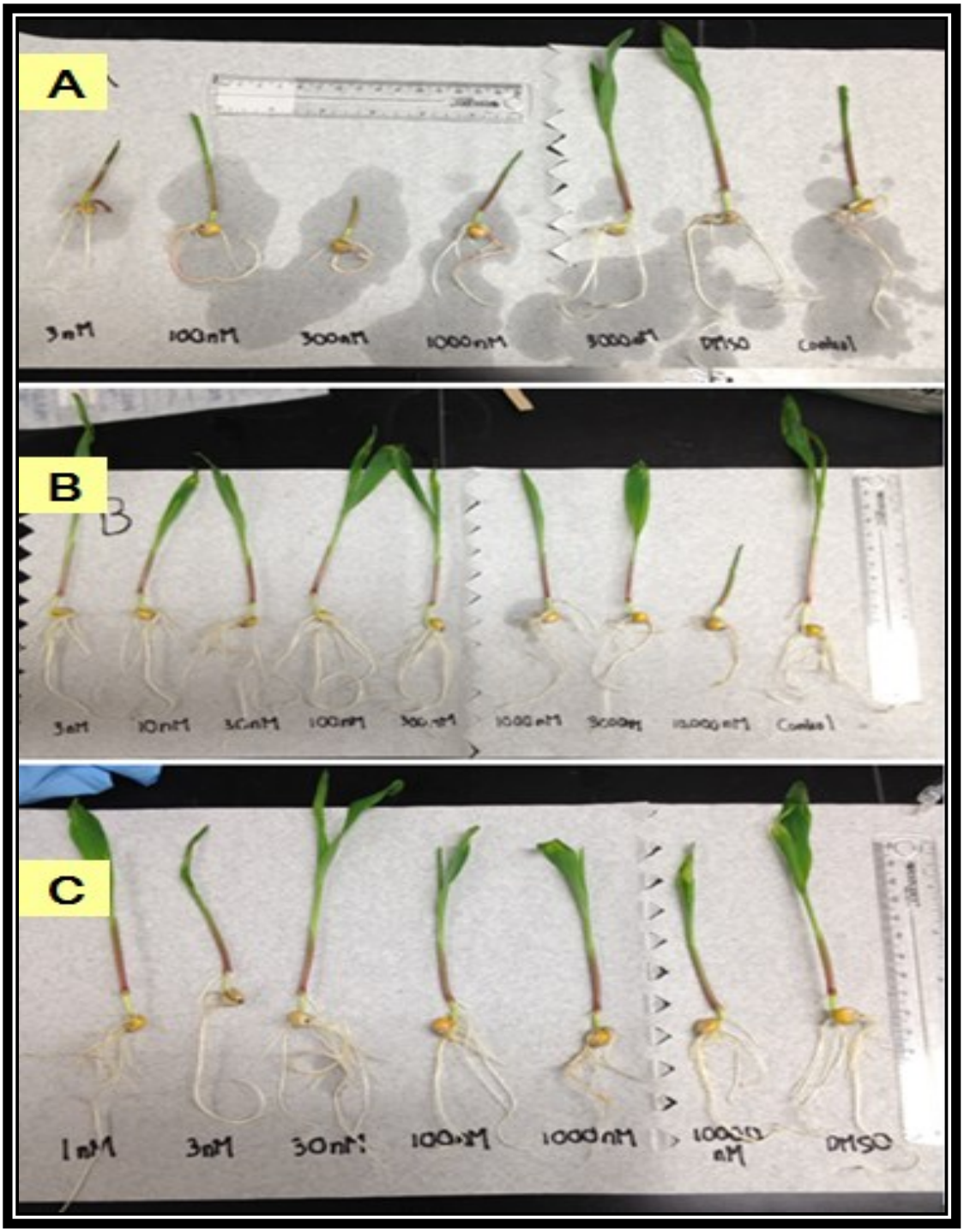

Figure 5: Images taken of the growing W64A+ seedlings 7 days after germination.

Analytical Graphs

Root Growth vs Rapamycin Concentration

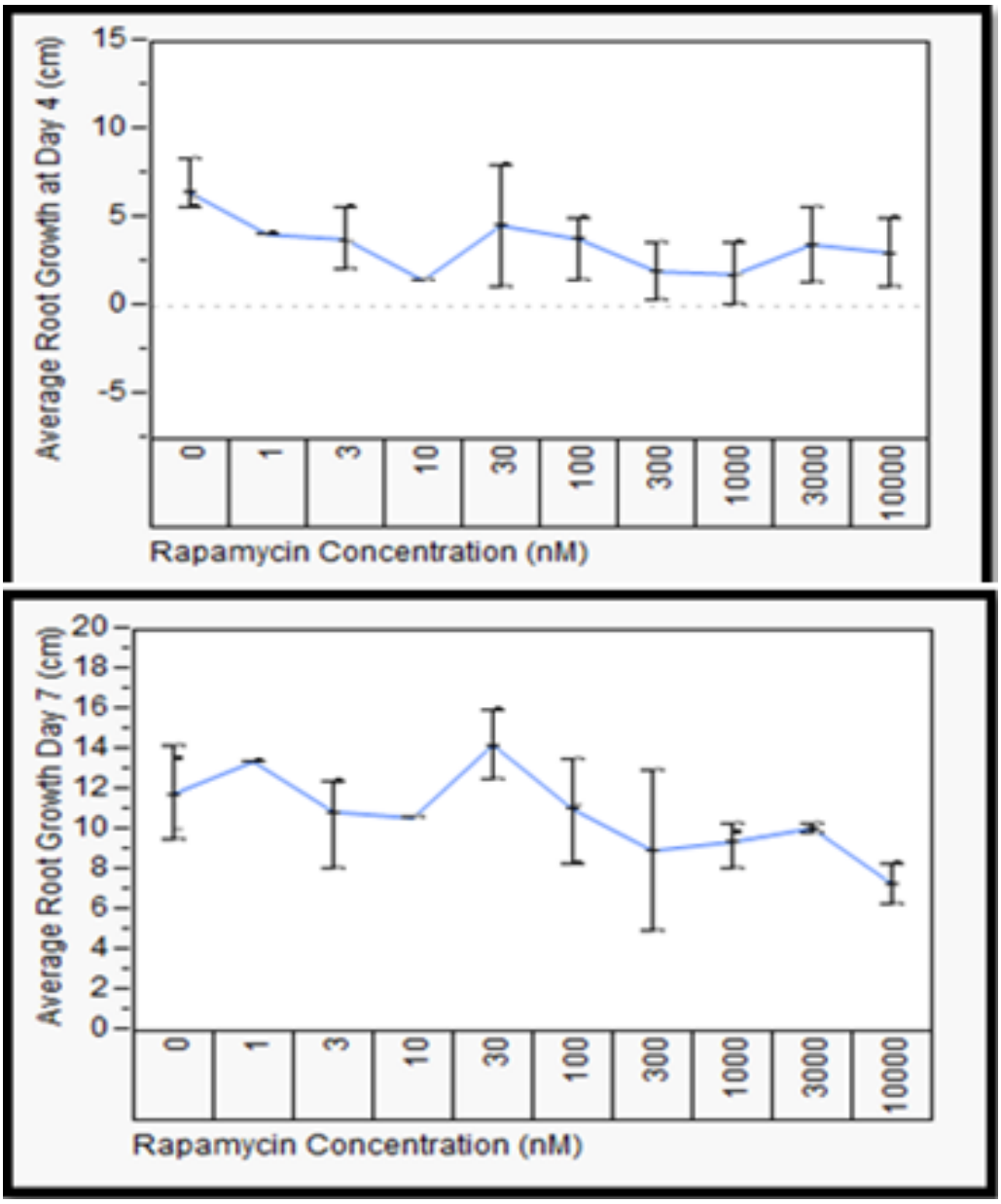

Figure 6: Plots of the average root growth at day 4 (top) and at day 7 (bottom) in correlation to increasing rapamycin concentrations.

Shoot Growth vs Rapamycin Concentration

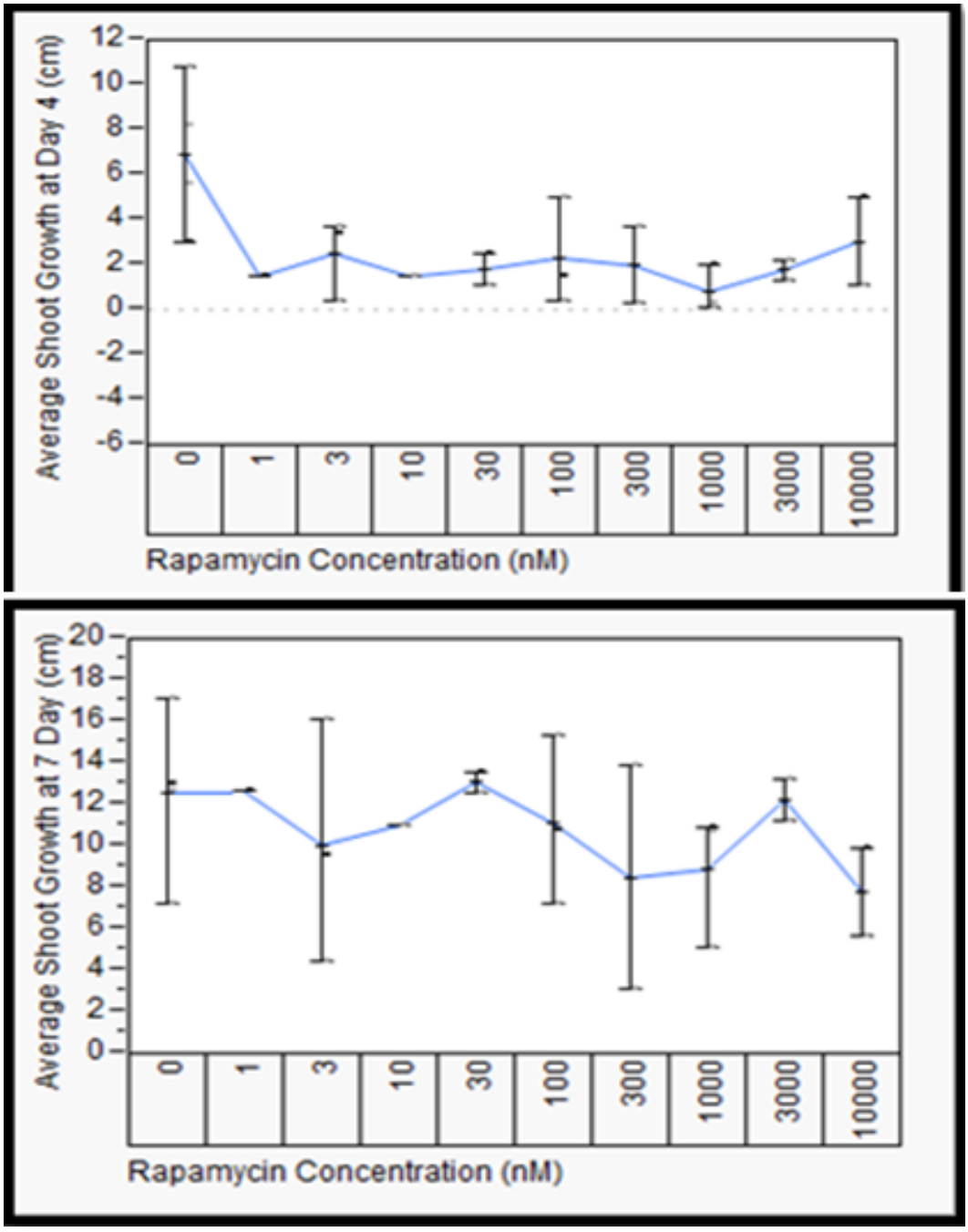

Figure 7: Plots of the average shoot growth at day 4 (top) and at day 7 (bottom) in correlation to increasing rapamycin concentrations.

After 4 days of germination, there was no significant trend, with the highest root growth rate occurring with no rapamycin present (6.15 cm in the DMSO control), and the lowest root growth rate occurring at approximately 10 nM rapamycin concentrations. These results did not support our hypothesis that the greatest root growth would occur at moderate concentrations of rapamycin. On the graph at the bottom of Figure 7, a small peak at 30 nM rapamycin reveals the trend of root growth at 7 days after germination. However, a paired t-test determined the difference between the growth rate at 0 nM rapamycin concentration (of either the DMSO or the water control) and 30 nM concentration as not statistically significant (P=0.1729).

Similar to the observed root growth, these data demonstrated the highest amount of shoot growth at 0 nM rapamycin concentration after 4 days (averaged 6.87 cm in the DMSO control). The shoot growth observed for all of the *Zea mays* samples exposed to rapamycin remained at low levels as indicated by the top graph. After 7 days, shoot growth remained highest at 0 nM and 30 nM rapamycin concentrations, and lowest at 1 nM, 300 nM, and 10 μM rapamycin concentrations.

Nucleic Acids Quantification

For the 3 nM sample in trial A, the RNA concentration was too low for qPCR (at 39.55 ng/ul). As for the assessment of nucleic acids purity as indicated by the 260/280 value, most of the samples possessed ratios of above 2.0, indicating high RNA purity, with the exception of the 10 nM sample in trial B (exhibiting 260/280 ratio of 1.47, indicating some possible protein contamination). However, measures of nucleic acid purity from the resulting 260/230 ratio (value range of 0.20 to 1.86) indicated a large presence of contaminants that absorbed at 230 nm for almost all samples.

Results of Nano Drop Spectrophotometer

TRIAL A					
Conc. (nM)	**ng/ul**	**A260**	**A280**	**260/280**	**260/230**
3	39.55	0.791	0.376	2.11	1.16
100	117.29	2.346	1.071	2.19	1.19
300	199.85	3.997	1.869	2.14	1.19
1000	248.06	4.961	2.098	2.36	0.57
3000	287.84	5.757	2.72	2.12	1.76
Control	298.01	5.96	2.826	2.11	1.49
DMSO	195.31	3.906	1.856	2.1	1.86
TRIAL B					
3	354.37	7.087	3.27	2.17	0.56
10	138.52	2.77	1.886	1.47	0.59
30	179.42	3.588	1.336	2.69	0.36
100	248.66	4.973	1.601	3.11	0.53
300	301.88	6.038	2.604	2.32	0.47
1000	215.96	4.319	1.775	2.43	0.35
3000	363.29	7.266	3.078	2.36	0.93
10000	204.99	4.1	1.597	2.57	0.32
Control	190.88	3.818	1.767	2.17	0.47
TRIAL C					
1	226.61	4.532	1.917	2.36	0.35
3	152.95	3.059	1.322	2.31	0.34
30	157.78	3.156	1.346	2.35	0.33
100	167.9	3.358	1.431	2.35	0.33
1000	214.58	4.292	1.847	2.32	0.38
10000	205.96	4.119	1.795	2.3	0.42
DMSO	119.11	2.382	0.808	2.65	0.2

Table 3: Measurements of RNA concentrations using a Nano drop Spectrophotometer.

qPCR Reaction

In the preliminary real time qPCR conducted of the cDNA samples from Trial B with ATG12 primers, all 8 *Zea mays* samples containing varying concentrations of rapamycin revealed insignificant amounts of amplified DNA (Table 4, No. 1-8). The cDNA of the seedlings exposed to 30 nM rapamycin that were expected to exhibit the highest level of amplification only exhibited a calculated concentration of 7.27 copies/ul (No. 3), a concentration lower than the no template control (NTC) sample, which was measured to be 10.3 copies/ul (No. 10). The RRB1 positive control, however, worked as expected and was shown to amplify the RRB gene in the seedling samples, exhibiting an average calculated concentration of 2.02E4 copies/ul (Table 4, No. 11-19). In comparison to the positive RRB1 control, the calculated concentration for the 30 nM cDNA sample was very low (No. 13). In fact, the ATG12 transcript was not amplified from any of the rapamycin treated maize cDNA. All of the calculated concentrations for the amplified cDNA were very low, indicating that the ATG12 primers had failed to amplify every one of the tested cDNA derived from the maize seedlings sample set. This result indicated that the ATG12 primers used were not appropriate for the qPCR reaction with our maize root sample set, and so we were not able to measure the autophagic expressions in the *Zea mays* samples. Identification of a working ATG primers set is necessary in order to produce a successful qPCR analysis.

No.	Name	Type	Ct	Conc. (copies/ul)	Calc. Conc (copies/ul)	% Var	Rep. Calc. Conc. (95% CI)
1	ATG (3-nM)	Unknown	37.56		8.34E+00		[2.555E+00 , 2.719E+01]
2	ATG (10-nM)	Unknown	37.48		8.78E+00		[2.701E+00 , 2.851E+01]
3	ATG (30-nM)	Unknown	37.78		7.27E+00		[2.204E+00 , 2.395E+01]
4	ATG (100-nM)	Unknown	38.26		5.35E+00		[1.585E+00 , 1.806E+01]
5	ATG (300-nM)	Unknown	37.23		1.03E+01		[3.200E+00 , 3.298E+01]
6	ATG (1E3-nM)	Unknown	37.47		8.82E+00		[2.716E+00 , 2.865E+01]
7	ATG (3E3-nM)	Unknown	36.95		1.23E+01		[3.874E+00 , 3.887E+01]
8	ATG (1E4-nM)	Unknown	37.23		1.03E+01		[3.214E+00 , 3.310E+01]
9	(Control)	Unknown	37.85		6.97E+00		[2.107E+00 , 2.305E+01]
10	(NTC)	NTC	37.23		1.03E+01		[3.207E+00 , 3.304E+01]
11	rrb1 (3-nM)	Positive Control	25.88		1.39E+04		[6.447E+03 , 2.977E+04]
12	Rrbl (10-nM)	Positive Control	23.59		5.92E+04		[2.817E+04 , 1.243E+05]
13	rrb1 (30-nM)	Positive Control	25.24		2.08E+04		[9.757E+03 , 4.424E+04]
14	rrb1 (100-nM)	Positive Control	24.18		4.09E+04		[1.940E+04 , 8.615E+04]
15	rrb1 (300-nM)	Positive Control	28.46		2.70E+03		[1.190E+03 , 6.134E+03]
16	rrb1 6 (1000-nM)	Positive Control	26.47		9.55E+03		[4.402E+03 , 2.073E+04]
17	rrb1 7 (3000-nM)	Positive Control	25.83		1.43E+04		[6.641E+03 , 3.062E+04]
18	rrb1 8 (10000-nM)	Positive Control	26.12		1.19E+04		[5.511E+03 , 2.565E+04]
19	rrb1 9 (Control)	Positive Control	26.59		8.84E+03		[4.061E+03 , 1.922E+04]
20	rrb1 10 (NTC)	NTC	28.18		3.23E+03		[1.431E+03 , 7.270E+03]
23	3	Standard	30.1	9.69E+02	9.49E+02	2.00%	[5.278E+02 , 1.707E+03]
25	5	Standard	22.75	9.69E+04	1.01E+05	4.20%	[6.973E+04 , 1.462E+05]
27	7	Standard	15.59	9.69E+06	9.49E+06	2.00%	[5.294E+06 , 1.702E+07]

Table 4: Report generated using Rotor-Gene Real-Time Analysis Software 6.0 for qPCR. The low concentrations observed in the unknown indicated that the ATG12 primers failed to amplify the autophagy gene in the DNA samples derived from seedlings' roots tissue. The positive control RRB1 primers amplified the RRB1 gene expression as expected.

PCR Results

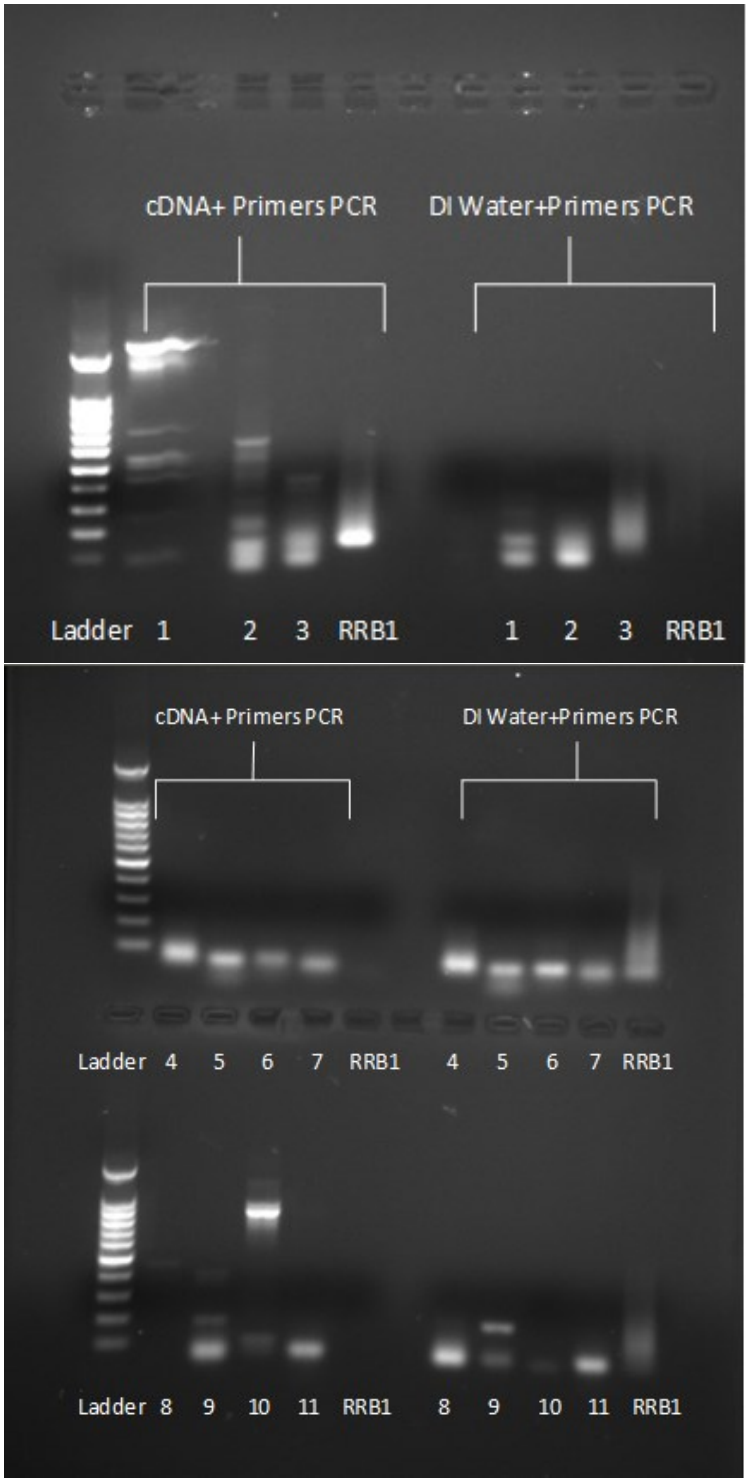

#	ATG Primers
1	ATG8a
2	ATG8b
3	ATG8c
4	ATG3a
5	ATG4a
6	ATG4b
7	ATG5a
8	ATG8d
9	ATG8e
10	ATG9
11	ATG10

Figure 8: 1% Agarose results of cDNA on the left side and DI water control on the right side testing 11 different ATG primer sets against a positive control RRB1. Each ATG primers possess complimentary sequences for variations of the expressed autophagy gene in the cDNA samples.

Because the ATG8 primer failed to amplify a specific product all 11 primer pairs were tested by conventional PCR to determine which ones failed to amplify a product of the expected size. In Figure 8, the first set of PCR electrophoresis conducted to identify a working ATG primers set for autophagy genes expressed in *Zea mays* root samples only revealed two possible candidates for a working primer pair, ATG8e and ATG9. Complimentary ATG primers were expected to reveal a single heavy band, but the results illustrated in the electrophoresis gels revealed either smears or blurred bands, shown in PCR electrophoresis of ATG8a, ATG8b, ATG8c, ATG3a, ATG4a, ATG4b, ATG5a, ATG8d, and ATG10. From Figure 8, there appeared to be possible interactions between the ATG 8e (#8) and the ATG9 (#10) primer sets. The identities of the bands presented in these lanes, however, are still unclear due to the vague band in lane 8 and the smear observed in lane 10 (Figure 8).

An additional PCR was conducted to confirm the specificity of primers ATG8e and ATG9 to detect autophagy gene expression in rapamycin treated *Zea mays* cDNA samples. In the repeated PCR electrophoresis results for the primers ATG8e and ATG 9 shown in Figure 9, there was a smear on the positive control RRB1 for both the cDNA samples and the negative control deionized water samples. The final result concerning the annealing specificity of the ATG primers to the *Zea mays* autophagy genes, consequently, remained inconsistent. Based on these unreliable PCR electrophoresis data indicating the primers' low reactivity to the sample cDNA, a working qPCR analysis could not be conducted to determine the autophagy expression level for the rapamycin treated *Zea mays* samples.

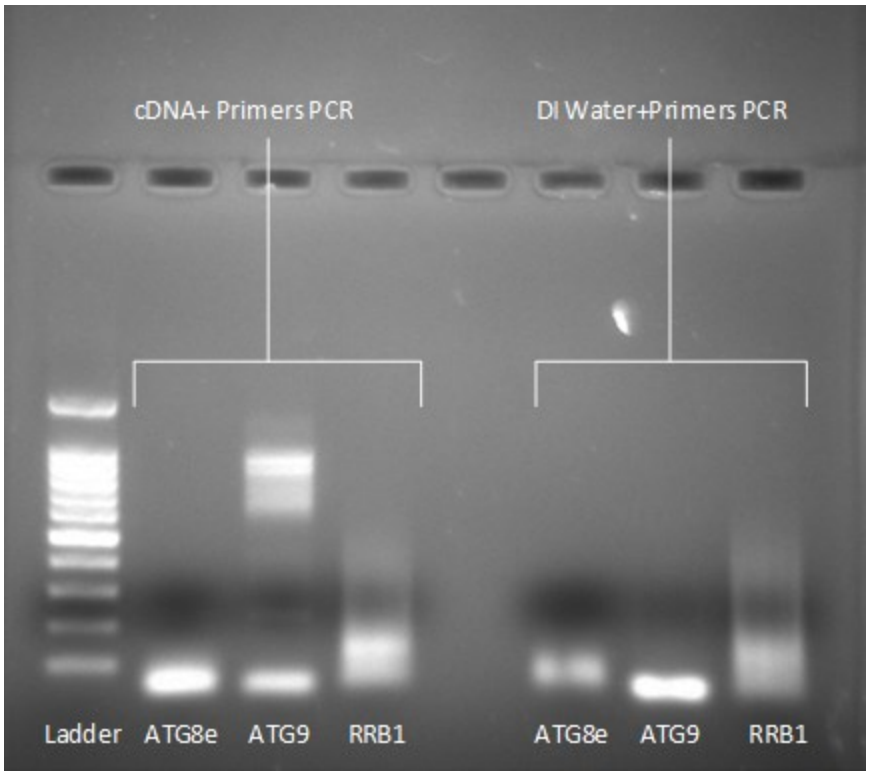

Figure 9: 1% Agarose results of cDNA on the left side and DI water control on the right side with ATG8e and ATG9 primer set along with positive control RRB1. Based on the presence of only one band on the second lane, ATG8e failed to amplify the seedling's cDNA. The third lane containing ATG9 exhibited a smear of several bands that suggested contamination of the primers sample. Furthermore, the RRB1 lanes in both the fourth and eighth lanes also exhibited smears, indicating unreliable agarose results.

CHAPTER FOUR

Discussion and Conclusion

This experiment was conducted to analyze the influence of rapamycin at varying concentrations on the early growth of maize seedlings through phenotypic observations and qPCR of extracted root cDNA. The initial hypothesis predicted that the *Zea mays* seedlings would exhibit a nutrient deficient response with exposure to rapamycin. Consequently, seedlings roots were expected to demonstrate faster growth rate with exposure to moderate concentrations of rapamycin in comparison to the wild type, and at higher levels of rapamycin concentration, the rate of root growth was expected to decline due to rapamycin's toxicity at high concentration. Observations of the growing *Zea mays* seedlings did not follow this trend initially. The rate of root growth documented 4 days after planting was highest at 0 nM of rapamycin, and then steadily declined except for a small but statistically insignificant peak at 30 nM concentration of rapamycin.

After 7 days of germination, despite exhibiting a peak in root growth at moderate concentrations of rapamycin, this result was still statistically insignificant based from the paired t test calculations. The hypothesis also predicted that the induced nutrient stress response was caused by rapamycin's interruption of the TOR-kinase pathway through the formation of an inhibitory complex with FKBP12 and TOR protein, resulting in autophagy induction at the *Zea mays* seedlings' root tips to increase root growth. Past studies had revealed rapamycin's ability to induce autophagy in photosynthetic organisms, such as in the *Chlamydomonas reinhardtii* model, evidenced through increased vacuole size induced by nutrient deprivation (Crespo et al., 2005).

Rapamycin's Influence on Root Growth Observation

The comparison of root growth made between the maize seedlings treated with different rapamycin concentrations in the three trials was measured from two sets of photographs using the ImageJ™ program (Figure 4 and Figure 5). The first set of photographs was taken 4 days after planting, and the second set of photographs was taken 7 days after planting. The root lengths of each of the maize seedlings were measured and plotted as Root Length vs. Rapamycin Concentration for each day of observation.

Discussion of Root Growth at 4 Days after Planting

In the analytical graph for Root Growth vs. Rapamycin Concentration (Figure 6, top), the plotted trend exhibited a high average initial rate of root growth at 0 nM rapamycin concentration for both the DMSO and deionized water control *Zea mays* seedlings, averaged at 7.40 cm for the DI water control and 6.15 cm for the DMSO control. Figure 6 indicated the highest rate of root growth in the seedlings exposed to rapamycin concentration between the range of 10 nM to 100 nM in both the 4th and the 7th day after planting. As rapamycin was gradually introduced, the observed root lengths steadily decreased (averaged 4.09 cm at 1 nM, 4.39 cm at 3 nM, and 4.16 at 10 nM). Then, a small sudden peak at 30 nM was observed, averaged at 5.79 cm measured root length. However, this minor peak in root growth at 30 nM rapamycin was insignificant according to the paired t-test between the average root growth at 0 nM (DMSO control) and the average root growth at the 30 nM peak ($t = 0.0497$, $P = 0.9684$). As the seedlings were exposed to higher levels of rapamycin, the rate of measured root length remained a steady low constant with the shortest root growth averaged to 2.32 cm at 1000 nM. While the rate of root growth did show a gradual decline as rapamycin concentration

increased from 0 to 10 μM, the peak growth at 30 nM was too insignificant to observe the increase in root growth at this concentration. Therefore, the original hypothesis predicting an increased root growth at moderate concentrations of rapamycin was not supported by the data obtained for the experimental *Zea mays* seedlings.

The high variation observed from the high initial rate of root growth demonstrated by the seedlings grown in rapamycin lacking media may be due to the lack of observable mold at the early phases of germination in comparison to the other seedlings (Table 1). No mold was documented for the viable DMSO and DI water control seedlings in all three trials. Molds were observed on 3 nM, 100 nM, and 300 nM rapamycin samples in Trial A, 10 nM and 30 nM rapamycin samples in Trial B, and 1 nM rapamycin sample in Trial C. Furthermore, the seedlings grown at 10-nM rapamycin exhibited a slow root growth, which did not follow the trend described by the initial hypothesis. However, since the 10 nM rapamycin seedling from trial B was the only 10 nM seedling that germinated, the root length data obtained at this rapamycin concentration was also insufficient for reliable analysis (10 nM seedlings from trial A and C failed to germinate due to mold contamination); evidence of some mold contamination based on Table 1 was observed in the 10 nM seedling in trial B as well, which may have further influenced the results obtained. Root growth comparison between the two controls, DMSO and DI water, also indicated a reduced rate of root growth in the DMSO control (6.15 cm) in comparison to the DI water control (7.40 cm). Past studies had demonstrated evidences of 50% reduction in plant growth in high concentration of DMSO (≥ 0.8%; Schmitz et al., 1969). Consequently, the fairly high concentration of DMSO (0.75%) in the DMSO control seedlings maybe responsible for this observation

Discussion of Root Growth at 7 Days after Planting

The graph of Root Growth vs. Rapamycin Concentration after 7 days of germination revealed an increase in root growth occurring in maize seedlings grown in moderate concentrations of rapamycin (Figure 6, bottom). This observed data followed more closely to the initial hypothesis that predicted a positive trend in root growth at moderate concentrations of rapamycin followed by decline in root growth as the seedlings were exposed to higher levels of rapamycin concentrations. The rates of root growth in seedlings that were exposed to 0 nM of rapamycin appeared to fall behind in comparison with the seedlings that were exposed to moderate levels of rapamycin, (averaged 13.86 cm for the control samples containing DMSO and 9.78 cm for the deionized water control samples). While the rates of root growth in the control rapamycin-free samples were initially high relative to the rapamycin treated seedlings 4 days after germination, the reduced root growth after 7 days of germination suggested evidence of lower autophagic expressions in the control seedlings. In regard to the difference in rates of root growth between the DMSO and the deionized water controls, the presence of mold observed in the deionized water control maybe a contributing factor for the discrepancy in rates of root growth between the two control types. At moderate concentrations of rapamycin, the rates of root growth appeared to be faster than the seedlings exposed to higher levels of rapamycin concentration, averaging 13.43 cm at 1 nM concentrations, 10.93 cm at 3 nM concentrations, 10.62 cm at 10 nM concentrations, and 14.26 cm at 30 nM concentrations compared to 11.06 cm at 100 nM concentrations, 8.99 cm at 300 nM, 9.43 cm at 1μM, 10.11 cm at 3 μM, and 7.33 cm at 10 μM. The plotted trend exhibited a peak in root growth at 30 nM rapamycin concentrations, after

which the rates of root growth appeared to progressively decline as rapamycin became more concentrated.

However, the increased root growth at 30 nM rapamycin remained insufficient to confirm the increase in root growth at moderate concentrations of rapamycin. The paired t-test analyzing the observed data between root growth measured at 0 nM rapamycin (DMSO) and the root growth measured at the 30 nM rapamycin peak determined the difference to be statistically insignificant ($P = 0.8880$, $t = 0.1777$). The presence of wide variations in the data obtained and the presence of mold were factors that may have contributed to this large variability. Consequently, the data obtained for the phenotypic observations were insufficient to predict the increased autophagic activities within rapamycin treated seedlings. Data from real time qPCR reactions remained necessary to confirm the increased trend of autophagic expressions in moderate concentration of rapamycin. The enhanced autophagic activities must be confirmed by testing for specific autophagy gene expression in the harvested root samples.

Discussion of Shoot Growth

The rates of shoot growth were also measured to observe for any trend that may correlate with the trend in root growth. Due to the suspicion for increased autophagic activities in seedlings treated with moderate concentrations of rapamycin, the rates of shoot growth were expected to demonstrate slower rates of shoot growth in comparison to the control seedlings. The rates of shoot growth observed after 4 days of germination indicated faster rates of shoot growth at 0 nM concentrations of rapamycin in comparison to the rapamycin treated seedlings (averaging 6.87 cm for the DMSO controls and 6.94 cm for the deionized water controls). However, the variations observed in the control

sample measurements were large, as indicated by the large range in the shoot lengths collected for control seedlings. For the rapamycin treated seedlings, the rates of shoot growth appeared to remain at a constant rate despite the increased in rapamycin concentrations, as evidenced in the top graph of Figure 7. In the observations recorded 7 days after germination, the control seedlings still maintained a high rate of shoot growth (averaging 12.86 cm for the DMSO controls and 12.21 cm for the deionized water controls). The graph also indicated peaks in shoot growth at 30 nM and at 3 μM rapamycin concentrations (averaging 13.08 cm at 30 nM and 12.23 cm at 3 μM). The large variations in the majority of the recorded lengths of shoot growth (Figure 7, bottom) made it difficult to determine any distinct trend in the correlations between shoot growth and increasing rapamycin concentrations.

qPCR and PCR Electrophoresis Analysis of Maize Seedlings

While phenotypic observations for the trends in root growth vs. rapamycin concentration can only provide indirect observations of increased autophagic processes, quantification of autophagy gene expression in each sample seedlings through qPCR allows a more direct and accurate measurements of autophagy gene expression in response to increasing rapamycin concentrations. Since the autophagy pathway involved intracellular activities that cannot be observed externally, the phenotypic observations of root growth were not a complete indication of the autophagy processes. To measure the autophagy expression, root tissue samples from each viable seedling were harvested for RNA extraction and reverse transcription to produce cDNA samples, which were used to test several gene-specific primers through qPCR to determine if autophagy was upregulated.

However, the first qPCR data obtained from reaction of cDNA extracted (Sample set B) with ATG12 primers did not show any amplification (Table 4), indicating a failure of the ATG12 primers to anneal with autophagy gene sequences in the sample cDNA. Since the ATG12 primers did not function properly, a series of PCR gel electrophoresis was performed using one of the root sample cDNA (100-nM, Sample set B) to test all of the available ATG primers in stock for the purpose of identifying a working ATG primer pair that would anneal to the W64A+ cDNA. Excluding primer pair ATG 12 that was demonstrated not to work in the qPCR reaction, 11 other ATG primer pairs was tested (ATG8a, ATG8b, ATG8c, ATG3a, ATG4a, ATG4b, ATG5a, ATG8d, ATG8e, ATG9, and ATG10) against a positive controlled standard RRB1, and negative control which contain deionized water instead of the W64A+ cDNA sample.

The electrophoresis results revealed that a majority of the ATG primers (Figure 8 lane # 3, 4, 5, 6, 7, 9, and 11) do not anneal to the cDNA sample. Possible contamination of the primers may also contribute to the smearing or presence of multiple bands (#1, 2) as shown in the aragose gel image in Figure 8. Out of these 11 primers, only 2 primer pairs appeared to interact with the sample cDNA to produce heavier bands in comparison to the rest of the samples (#8, 10). However, the positive control RRB1 did not produce a band in this gel electrophoresis, so the ability of the primers to anneal to the cDNA is uninterpretable and thus must be further confirmed through another PCR gel electrophoresis with just primer set 8 and 10 (ATG8e, ATG9). The result of this gel electrophoresis, as illustrated in Figure 9, showed no band for ATG8e, and only a smear for ATG9 and RRB1. Consequently, this result is still inconclusive and the smeared band

produced by the primer ATG9 rendered it unsuitable for conducting qPCR with the rest of the W64A+ root cDNA sample.

Conclusion

The documented rate of W64A+ *Zea mays* root growth did provide some evidence of increased root growth in seedlings exposed to moderate levels of rapamycin. However, this observation was insufficient to confirm the increased autophagy expression in *Zea mays* seedlings treated with moderate rapamycin concentrations predicted by the initial hypothesis. The low number of samples in each group, high variability within the data set, and the lack of reliable qPCR results rendered it difficult to analyze the induction of autophagy in the seedlings. In conclusion, no definite conclusions can be inferred on rapamycin's influence on the autophagy process in *Zea mays* seedlings from this experiment.

The reason for the inefficient binding of the ATG primers during this experiment may be due to the high genetic diversity of maize. The primer sequences used in the experiment were obtained from 12 primer sets that were developed by Chung et al. (2009), who had designed the primers using the B73 maize inbred sequence. Additionally, the W64A+ maize line used in this experiment may possess single nucleotide polymorphisms or insertion-deletion differences from the B73 maize inbred sequence that the ATG primers had been designed for, resulting in poor amplification of the autophagy genes in the W64A+ root samples used.

Another external factor that influenced the documented data during the course of the experiment was the presence of mold growing on the W64A+ seedlings. Mold growth on the developing seedlings may release damaging toxins and limiting the available nutrients

for the growing maize seedlings, thus resulting in a negative effect on the seedlings' growth. Efforts to minimize mold contamination consisted of pretreating the *Zea mays* kernels with LATITUDE^{TM} and germinating the kernels under a hooded vent. Despite precautionary measures, presence of mold contamination still rendered 24% of the original sample unusable. In future experiments, a larger sample size is necessary to account for the variability of data caused by mold contamination.

Limitations in the digital image analysis and propagation of errors during the RNA extraction process may also have contributed to the increased variability in the data obtained. At the fourth day after planting, measurements of root lengths were made using the ImageJ^{TM} program through analysis of digital photographs taken. However, the rapid root growth of maize seedlings at this stage led to increasing space restriction within the media tube, forcing the roots to coil around the circumference of the media tube to accommodate for its increasing length. Since ImageJ^{TM} can only analyze 2-dimensional image, the coiling of the seedlings' growing roots made it difficult to accurately measure the root lengths. This problem was less pronounced at 7 days because the seedlings could be removed from the tubes prior to photographing.

During the RNA extraction and cDNA preparation processes, the nucleic acid root sample extracted from the harvested seedlings experienced high risk of degradation if the sample was not kept cold. By subjecting the nucleic acid samples to bench work and fluctuation in temperatures during pipetting procedure, errors caused by contamination and loss of RNA or cDNA maize samples could have increased. The presence of contamination was suggested based on the results of the NanoDrop Spectrophotometer, where measures of nucleic acid purity from the 260/230 ratio indicated a large presence

of contaminants that absorbed at 230 nm for the majority of the seedlings' RNA root samples (Table 3). Thus, the data obtained from this experiment are not reliable and must be verified with additional experiments. However, the phenotypic data observed and the prepared cDNA samples obtained will be helpful for future experiments involving analysis of the rapamycin induced autophagic pathway in the W64A+ maize line.

REFERENCES

Agredano-Moreno, L., Reyes de la Cruz, H., Martínez-Castilla, L., & Sánchez de Jiménez, E. (2007). Distinctive expression and functional regulation of the maize (Zea mays L.) TOR kinase ortholog. *Molecular Biosystems*, *3*(11), 794-802.

Anderson, G. H., Veit, B., & Hanson, M. R. (2005). The Arabidopsis AtRaptor genes are essential for post-embryonic plant growth. *BMC Biology*, *31-11*. doi:10.1186/1741-7007-3-12

Chang, Y., & Neufeld, T. (2009). An Atg1/Atg13 complex with multiple roles in TOR-mediated autophagy regulation. *Molecular Biology Of The Cell, 20*(7), 2004-2014. doi:10.1091/mbc.E08-12-1250

Chung, J., Kuo C, J., Crabtree G, R., & Blenis, J. (1992). Rapamycin-Fkbp Specifically Blocks Growth-Dependent Activation Of And Signaling By The 70 Kd S6 Protein Kinases. *Cell*, *69*(7), 1227-1236.

Chung, T., Suttangkakul, A., and Vierstra, R.D. (2009). The ATG autophagic conjugation system in maize: ATG transcripts and abundance of the ATG8-lipid adduct are regulated by development and nutrient availability. *Plant Physiol 149*, 220-234.

Crespo JL, Diaz-Troya S, Florencio FJ (2005) Inhibition of target of rapamycin signaling by rapamycin in the unicellular green alga Chlamydomonas reinhardtii. *Plant Physiol* 1*39*: 1736–1749.

Dobrenel, T., Marchive, C., Sormani, R., Moreau, M., Mozzo, M., Montane, M., Menand, B., Robaglia, C., Meyer, C. (2011). Regulation of plant growth and metabolism by the TOR kinase. *Biochemical Society Transactions*, *39*(Part 2), 477-481.

Faivre, S. (2006). Chemical structure of rapamycin and rapamycin derivatives. Graphic. Nature Reviews: *Drug DiscoveryWeb*. 11 Apr 2013. <http://www.nature.com/nrd/journal/v5/n8/box/nrd2062_BX2.html>.

Fumarola, C., La Monica, S., Alfieri, R., Borra, E., & Guidotti, G. (2005). Cell size reduction induced by inhibition of the mTOR/S6K-signaling pathway protects Jurkat cells from apoptosis. *Cell Death And Differentiation, 12*(10), 1344-1357.

Li, F., & Vierstra, R. (2012). Autophagy: a multifaceted intracellular system for bulk and selective recycling. *Trends In Plant Science*, *17*(9), 526-537. doi:10.1016/j.tplants.2012.05.006

Loewith, R., & Hall, M. (2011). Target of rapamycin (TOR) in nutrient signaling and growth control. *Genetics, 189*(4), 1177-1201. doi:10.1534/genetics.111.133363

Dennis, P., Fumagalli, S., & Thomas, G. (1999). Target of rapamycin (TOR): balancing the opposing forces of protein synthesis and degradation. *Current Opinion In Genetics & Development*, *9(*1), 49-54.

Harding, M. A., Galat, A. (1989). A receptor for the immuno-suppressant FK506 is a cis-trans peptidyl-prolyl isomerase. *Nature*, *341*(6244), 758.

Mahfouz, M., Kim, S., Delauney, A., & Verma, D. (2006). Arabidopsis TARGET OF RAPAMYCIN interacts with RAPTOR, which regulates the activity of S6 kinase in response to osmotic stress signals. *The Plant Cell, 18*(2), 477-490

Menand, B., Desnos, T., Nussaume, L., Berger, F., Bouchez, D., Meyer, C., & Robaglia, C. (2002). Expression and disruption of the Arabidopsis TOR (target of rapamycin) gene. *Proceedings Of The National Academy Of Sciences Of The United States Of America*, *99*(9), 6422-6427.

Oshiro, N., Yoshino, K., Hidayat, S., Tokunaga, C., Hara, K., Eguchi S., Avruch J.,Yonezawa K. (2004). Dissociation of raptor from mTOR is a mechanism of rapamycin-induced inhibition of mTOR function. *Genes To Cells: Devoted To Molecular & Cellular Mechanisms*, *9*(4), 359-366.

Rohde, J., Heitman, J., & Cardenas, M. E. (2001). The TOR kinases link nutrient sensing to cell growth. *Journal Of Biological Chemistry*, *276*(13), 9583-9586.

Thompson, A. R., Doelling, J. H., Suttangkakul, A., & Vierstra, R. D. (2005). Autophagic nutrient recycling in Arabidopsis directed by the ATG8 and ATG12 conjugation pathways. *Plant Physiology* (*Rockville), 138*(4), 2097-2110.

Wood, A.J. and Roper, J. (2000). A Simple and Nondestructive Technique for Measuring Plant Growth and Development. *American Biology Teacher*, v62 n3 p215-17.

Xiong, Y., & Sheen, J. (2012). Rapamycin and glucose-target of rapamycin (TOR) protein signaling in plants. *The Journal Of Biological Chemistry, 287*(4), 2836-2842. doi:10.1074/jbc.M111.300749

Yoshimoto, K., Hanaoka, H., Sato, S., Kato, T., Tabata, S., Noda, T., & Ohsumi, Y. (2004). Processing of ATG8s, ubiquitin-like proteins, and their deconjugation by ATG4s are essential for plant autophagy. *Plant Cell*, *16*(11), 2967-2983.

Zhang, S., Lawton, M. A., Hunter, T., & Lamb, C. J. (1994). Atpk1, a novel ribosomal protein kinase gene from Arabidopsis: I. Isolation, characterization, and expression. *Journal Of Biological Chemistry*, *269*(26), 17586-17592.